Solvent Effects on the Growth and Steric Stabilization of Copper Metallic Nanoparticles in AOT Reverse Micelle Systems

Christopher L. Kitchens, M. Chandler McLeod, and Christopher B. Roberts*

Department of Chemical Engineering, Auburn University, Auburn, Alabama 36849

Received: May 21, 2003; In Final Form: August 12, 2003

Organic and inorganic reactions within the aqueous cores of water-in-oil AOT reverse micelle systems are viable methods for the production of nanomaterials of controllable composition and geometry while maintaining narrow size distributions. Considerable research has been done in order to better understand the governing features which comprise the AOT reverse micellar system, particularly stability and the intermicellar exchange of the contents within the aqueous core. The intermicellar exchange rate is affected by the bulk solvent type, the contents dissolved within the core, and the size of the reverse micelle or the water content, referred to as the *W* value, where *W* is the molar ratio of the water to AOT surfactant concentrations. Synthesis of nanomaterials within the AOT reverse micelle system is a strong function of the intermicellar exchange process and the factors mentioned previously. This study examines the effects of varying the bulk liquid solvent and the *W* value on the growth rate and ultimate particle size of copper nanoparticles produced via reduction of $CuAOT_2$ within the micelle core. Particle growth is measured in-situ using time-resolved UV−Vis absorbance spectroscopy, and the particle size is determined by both UV−Vis measurements and TEM analysis. A total interaction energy model is implemented to represent the attractive van der Waals forces acting between the metallic particles and the repulsive osmotic and elastic forces which result from the surfactant tail−tail and solvent−tail interactions responsible for the steric stabilization of the metallic particles within the microemulsion. The model is able to predict the ultimate particle sizes obtained experimentally for copper and silver nanoparticles synthesized using a variety of bulk liquid solvents including isooctane, cyclohexane, and *n*-alkanes ranging from pentane to dodecane.

Introduction

There has been a great deal of work performed in order to improve the fundamental understanding of the AOT reverse micelle system.[1−9] However, conflicting opinions on some aspects of the AOT system remain, particularly the underlining factors controlling the synthesis of nanomaterials through aqueous phase reduction reactions within the AOT reverse micelle core. Previous work done with the water/alkane/AOT surfactant system has shown that the bulk solvent and water content, $W = [H_2O]/[AOT]$, have a profound effect on the intermicellar exchange of the water cores and the kinetics of nanoparticle formation.[7,10−18] This study of copper nanoparticle synthesis within AOT reverse micellar systems explores the effects of *W* and the bulk alkane solvent type on the particle growth rate and the ultimate particle size obtained. We have also applied an interaction energy model to describe the forces between the metallic copper nanoparticles coated with AOT surfactant dispersed within alkane solvents in order to predict the ultimate particle size obtained from this synthesis. The model was similarly employed for the synthesis of silver particles in similar media.

Studies of the water-in-oil microemulsion system have presented a mechanism of intermicellar exchange of the water core contents[2−5] as a rate-determining step in particle formation.[6,7] Robinson and co-workers[4] presented a comprehensive study on the water/alkane/AOT system where the rate of micellar exchange k_{ex} was measured as a function of the water content *W*, the AOT concentration, temperature, and the bulk solvent type. The results from their study reveal that k_{ex} decreases with increasing water content for $W = 10$, 15, 20, and 30; k_{ex} is independent of AOT and reactant concentration; k_{ex} increases with an increase in temperature; and k_{ex} increases slightly with carbon number for pentane through dodecane in addition to a significant decrease in k_{ex} for the corresponding cyclic compounds, particularly cyclohexane. The dependency of k_{ex} on the bulk solvent can be explained by the solvent interactions with the AOT tails where a more favorable interaction will allow for the solvent to insert itself within the surfactant tails, thus creating a more rigid micelle. Binks et al.[9] discuss the extent of oil penetration into the surfactant chain region, showing an increase in micelle rigidity with decreasing solvent chain length from C_{14} to C_7. Studies on particle formation have shown that underlying properties of the AOT reverse micelle system resulting from the water content and interactions between the bulk solvent and AOT surfactant tails significantly affect the particle growth rate and the ultimate particle size obtained.[7,13−17] In this paper, we will study the effects of solvent properties on the synthesis of copper nanoparticles in the AOT reverse micellar system through investigations of particle growth rates and the ultimate particle size obtained in each liquid solvent system.

Pioneering work by Lisiecki and Pileni[12] on the production of copper nanoparticles in the AOT reverse micelle system has set forth the methods for synthesis via reduction of the Cu^{2+} ion. The Cu^{2+} ion was introduced into the reverse micelle system by functionalization of the AOT ionic headgroup, replacing the

* Corresponding author. E-mail: croberts@eng.auburn.edu.

10.1021/jp0354090 CCC: $25.00
Published on Web 09/24/2003

Na^+ ion to form $Cu(AOT)_2$ surfactant. In Lisiecki and Pileni's work, it was noted that the bulk solvent and *W* value have a significant effect on the dynamics of nanoparticle production. In addition, a direct relationship between the size of copper nanoparticles in solution and the UV−Vis absorption spectra was revealed where a characteristic peak at a wavelength of 566 nm can be used to indirectly measure the copper nanoparticles diameter. The ratio of the absorbance at 566 nm and the absorbance off the peak at 500 nm (Abs_{566}/Abs_{500}) is correlated directly to the average particle diameter measured by TEM imaging techniques. This proves to be invaluable for the in-situ measurement of the copper nanoparticle diameter and thus allows time-resolved absorption measurements to be used to study the growth of the copper particles over time. From this absorption ratio we are able to perform a kinetic analysis on the particle synthesis and obtain the particle growth rates as well as the ultimate particle size obtained. Related in-situ time-resolved absorption studies have been done to study the kinetics of nanomaterial synthesis within AOT reverse micelle systems which include Ag, CdS, and ZnS particles.[7,10,14−16,19]

Modeling

The factors controlling the ultimate size and shape of particles grown within the reverse micelles remains an area of significant interest. One opinion that the reverse micelles act as a template for the production of particles has been suggested by nanoparticle synthesis in various geometries such as spheres and rods.[11,20] For materials such as CdS, ZnS,[15] and AgCl[17] it has been observed that the particle size is controlled by the size of the micelle. However, time-resolved studies on the formation of Cu nanoparticles by Cason et al.[18] have shown that, given adequate reaction time, the ultimate particle size obtained in the AOT/alkane reverse micelle system is independent of *W*, although the particle growth rate is a function of *W* and the bulk solvent type. This leads to an alternate theory that the particle sizes obtained are largely controlled by solvent stabilization of the particles where the surfactant acts as a stabilizing ligand. Johnston and co-workers have recently demonstrated that silver and gold nanocrystals, sterically stabilized by dodecanethiol ligands and dispersed in supercritical ethane, can be selectively separated according to size by adjusting the temperature and pressure of the system.[21] Therefore, the solvent strength of the supercritical phase can be adjusted to support various sized particles by adjusting the operating conditions of the system. As such, particle dispersibility is a function of the solvent strength where an increase in pressure or a decrease in temperature, raises the solvent density and ability to support larger particles.

In this work, a similar theoretical approach is used to examine solvent effects on the ultimate particle size that can be synthesized and stabilized in the AOT reverse micelle system. We have experimentally observed that adjusting the properties of the bulk solvent can induce a change in the growth rate and the ultimate particle size obtained, which will be explained through the solvation interactions between the surfactant tails and the bulk phase. The work by Shah et al.[21] set forth a model that takes a soft sphere approach to balance the attractive van der Waals force with steric repulsive forces to determine the total interaction energy. To model the metallic nanoparticle synthesis within the reverse micellar system, the soft sphere approach was modeled as a spherical metallic nanoparticle surrounded by an AOT monolayer with the alkyl tails interacting with the bulk solvent. The AOT encased metallic particle excludes the presence of the water in the model for simplification as well as the fact that typical synthesis begins with ∼2 nm diameter reverse micelles and results in ∼10 nm diameter particles. It is assumed that the amount of water present in the particle/surfactant system modeled is minimal and limited to the smallest amount necessary to hydrate the surfactant headgroups for particle stabilization. The total interaction energy is achieved by a simple summation of attractive and repulsive forces:

$$\Phi_{total} = \Phi_{vdW} + \Phi_{osm} + \Phi_{elas} \tag{1}$$

The repulsive energy contribution consists of an osmotic term, Φ_{osm}, and an elastic term, Φ_{elas}, which will be discussed later. The van der Waals attractive force, Φ_{vdW}, between two nanoparticles is a function of the particle radius *R*, the center to center separation *d*, and the Hamaker constant *A*.

$$\Phi_{vdW} = -\frac{A_{131}}{6}\left[\frac{2R^2}{d^2-4R^2} + \frac{2R^2}{d^2} + \ln\left(\frac{d^2-4R^2}{d^2}\right)\right] \tag{2}$$

The Hamaker constant A_{131} is a proportionality factor that accounts for two nanoparticles of the same material (component 1) interacting through a solvent (component 3) and is determined from pure component values by the following relationship:

$$A_{131} \approx (\sqrt{A_{11}} - \sqrt{A_{33}})^2 \tag{3}$$

The Hamaker constants for the metal nanoparticles are constant with $A_{11} = 1.723$ eV for copper and $A_{11} = 2.440$ eV for silver.[22] For the bulk fluid, A_{33} is calculated on the basis of Lifshitz theory by the following relation:[23]

$$A_{33} = \frac{3}{4}k_B T\left(\frac{\epsilon_3 - \epsilon_{vacuum}}{\epsilon_3 + \epsilon_{vacuum}}\right)^2 + \frac{3h\upsilon_e}{16\sqrt{2}}\frac{(n_3^2 - n_{vacuum}^2)^2}{(n_3^2 + n_{vacuum}^2)^{3/2}} \tag{4}$$

where ϵ is the dielectric constant, *n* is the refractive index, k_B is Boltzmann's constant, *T* is temperature, h is Planck's constant, and υ_e is the main electronic UV absorption frequency, typically assumed to be 3×10^{15} s^{-1}. Values for ϵ_{vacuum} and n_{vacuum} are assumed to be 1, while the ϵ and *n* for bulk liquids were obtained from the literature.[24]

The repulsive contribution to the total interaction energy originates from the "soft sphere" theory developed by Vincent et al.[25]and implemented by Shah et al.[21] where the following relations are proposed for the osmotic and elastic interaction terms.

$$\Phi_{osm} = \frac{4\pi R k_B T}{\upsilon_{solv}}\phi^2\left(\frac{1}{2} - \chi\right)\left(l - \frac{h}{2}\right)^2 \quad l < h < 2 \tag{5}$$

$$\Phi_{osm} = \frac{4\pi R k_B T}{\upsilon_{solv}}\phi^2\left(\frac{1}{2} - \chi\right)\left[l^2\left(\frac{h}{2l} - \frac{1}{4} - \ln\left(\frac{h}{l}\right)\right)\right] \quad h < l \tag{6}$$

$$\Phi_{elas} = \frac{2\pi R k_B T l^2 \phi\rho}{MW_2}\left\{\frac{h}{l}\ln\left[\frac{h}{l}\left(\frac{3 - h/l}{2}\right)^2\right] - 6\ln\left(\frac{3 - h/l}{2}\right) + 3\left(1 - \frac{h}{l}\right)\right\} \quad h < l \tag{7}$$

$$h = d - 2R \tag{8}$$

Here again, *R* is the particle radius and *d* is the center-to-center separation, and from eq 8 *h* is the separation distance from the particle surfaces. As will be seen from the interaction energy diagrams, this separation distance at a minimum energy will

determine the dispersibility of the particles. It must also be noted that the repulsive forces are independent of the particle material and do not contribute to the total interaction energy until the separation distance is less than twice the ligand length l. To obtain the ligand volume fraction, ϕ, the AOT was modeled as a cylindrical structure extending from the particle surface with a headgroup cross-sectional area of 75 Å^2 and a length of 9.1 Å[1] with a 90% surface coverage by the following equation:

$$\phi = 0.90\left(\frac{3R^2 l}{(R+l)^3 - R^3}\right) \tag{9}$$

This is a rough approximation due to the neglect of factors such as the actual surface coverage, the known cone-shaped structure of AOT, and the overlap of the surfactant tails, especially in the region of $h < 2l$ where repulsive forces come into play.

For the osmotic repulsion term υ_{solv} is the molecular volume of the solvent, and χ is the Flory−Huggins interaction parameter which is function of the Hildebrand solubility parameters δ_i:

$$\chi = \frac{\bar{v}_3}{RT}(\delta_3 - \delta_2)^2 \tag{10}$$

where R is the ideal gas constant and $\bar{v}_3$ is the molar volume of the solvent. The solubility parameter for the solvent is related to the cohesive energy density $E_3^{coh}$and can be calculated by the following relation:[26]

$$\delta_3 = \sqrt{E_3^{coh}} = \sqrt{\frac{\Delta H_3^{v} - RT}{\bar{v}_3}} \tag{11}$$

where ΔH_3^{v} is the enthalpy of vaporization and was obtained from the literature for each solvent.[24] The values listed were measured at the boiling point of the liquid; in order to account for the temperature effects and determine the solubility parameter at 20 °C, Watson's correlation for latent heat was implemented:[27]

$$\Delta H_{20°C} = \Delta H_{bp}\left(\frac{T_C - 20\ °C}{T_C - T_{bp}}\right)^{0.38} \tag{12}$$

The solubility parameter for AOT must be estimated using a group contribution method typically implemented for polymer solutions where a molar attraction constant is assigned for each chemical group in the surfactant tail. There are several group contribution methods available;[26] however, in this case the Hoy method was implemented to obtain $\delta_2 = 517.52$ (MPa)$^{1/2}$. The osmotic repulsion term deals solely with the interactions of the surfactant tails with themselves and the bulk solvent. The key terms which determine the intensity of the osmotic repulsive energy are ϕ, υ_{solv}, and in particular χ. These terms are significant in determining the repulsive forces due to the surfactant tail−tail and tail−solvent interactions which are responsible for particle stabilization and preventing agglomeration. The chi interaction parameter, χ, is representative of the solvent interaction between the AOT tails and the bulk solvent where solvation occurs when $\chi < 0.5$ and the solvent strength increases as χ decreases.[26] The elastic repulsion term contributes to the interaction energy in the range $h < l$ and represents the energy requirement for compression of the surfactant tails. The contribution can be calculated from eq 7 where ρ and MW_2 represent the surfactant density and molecular weight. The elastic term represents the surfactant tail−tail repulsion that occurs on compression of the tails and is largely a function of the surfactant density and volume fraction.

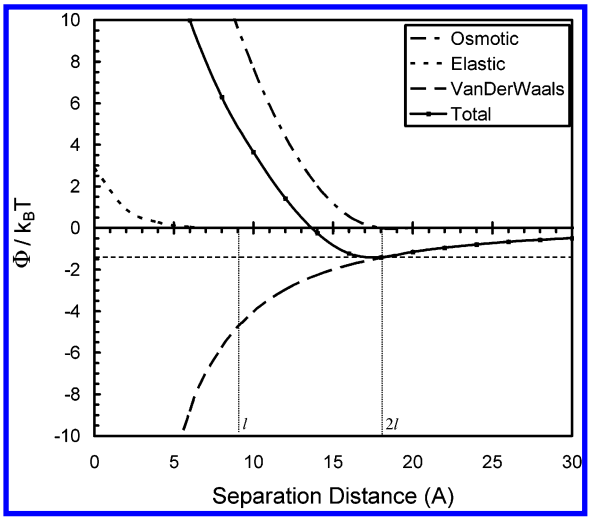

Figure 1. Contributions to the Total Interaction Energy Model for silver nanoparticles coated with AOT dispersed in hexane at 25 °C and 1 bar.

The contribution of each of the forces to the total interaction energy can be seen in Figure 1 as a function of the separation distance of the particles. The elastic term does not contribute greatly and it is the osmotic forces that more strongly influences the particle dispersion by countering the attractive van der Waals forces. Along the total interaction energy curve a minimum value exists that corresponds to an optimum position of the particles with respect to each other. A threshold energy of $-{}^3/_2 kT$ or greater is required to disperse the particles within the bulk solvent. Particle growth occurs through random exchange of micelle contents and will continue to grow until this threshold energy limit is reached. If particle growth occurs beyond an optimum size, the total interaction energy will drop below this threshold energy limit of $-{}^3/_2 kT$ and the particles will agglomerate and precipitate out of solution. In this case, the repulsive terms are insufficient to balance the attractive van der Waals forces, thereby resulting in an inability to disperse the particles. The total interaction energy can be calculated as a function of the separation distance for various particle sizes, solvents, temperatures, and pressures in order to determine the optimum operating conditions for particle growth.

Experimental Section

Materials. Sodium bis(2-ethylhexyl) sulfosuccinate (AOT) and DIUF water were obtained from Fisher Scientific and used without further purification. Anhydrous hydrazine 98%, isooctane, and other alkane solvents were purchased from Sigma Aldrich. The alkane solvents were stored over molecular sieves to remove any dissolved water. Copper AOT ($CuAOT_2$) was synthesized by two separate methods published previously,[12,28] where the sodium ion of the AOT headgroup was replaced by a Cu^{2+} ion to create the functionalized surfactant.

Particle Synthesis. The method for the synthesis of copper nanoparticles via $CuAOT_2$ reduction using hydrazine within a liquid-phase AOT reverse micelle system has been discussed previously.[18] The bulk liquid alkane solvents investigated included pentane, hexane, heptane, octane, decane, dodecane, isooctane, and cyclohexane. AOT and $CuAOT_2$ were added in a 10 to 1 ratio at concentrations of 1.1×10^{-1} M and 1.1×10^{-2} M, respectively. W values ($[H_2O]/[AOT]$) ranging from 3 to 15 were examined. Solutions were sonicated and purged with

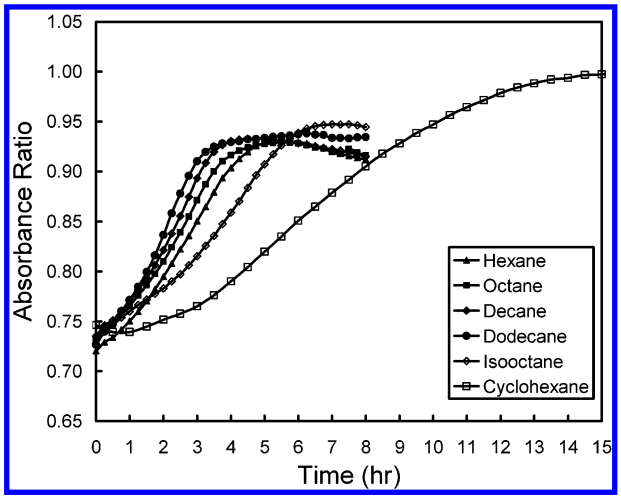

Figure 2. Copper nanoparticle growth curves measured in-situ by plotting the UV−Vis absorbance ratio (Abs_{500}/Abs_{566}) as a function of time using various alkane bulk solvents with $W = 5$, [AOT] = 0.1106 M, [$CuAOT_2$] = 0.01106 M, N_2H_4 = 3X [Cu]. The even-carbon-number alkanes are shown for clarity.

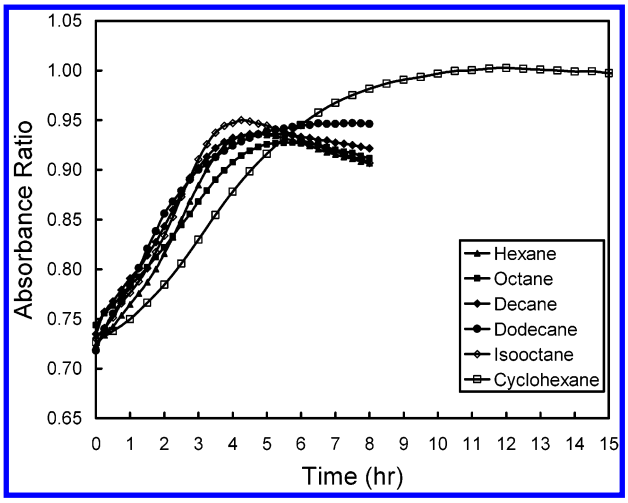

Figure 3. Cu nanoparticle growth curves measured in-situ by (Abs_{500}/Abs_{566}) as a function of time using various alkane bulk solvents with $W = 10$, [AOT] = 0.1106 M, [$CuAOT_2$] = 0.01106 M, N_2H_4 = 3X [Cu]. The even-carbon-number alkanes are shown for clarity.

nitrogen to remove oxygen from the system in order to prevent the formation of copper oxide. The solutions were then allowed to equilibrate, after which the hydrazine reducing agent was injected through a rubber septum at a concentration three times the copper concentration. A Varian, Cary 300 UV−Vis spectrophotometer was used to record the time-resolved absorbance measurements as the reaction proceeded.

Silver particles were produced in a similar manner to the copper particles with concentrations of AgAOT = 1.0×10^{-3} M, AOT = 9.9×10^{-2} M, $W = 10$ and reduction using hydrazine at 10 times excess of silver.[29] AgAOT surfactant was synthesized by an ion-exchange process similar to the synthesis of $CuAOT_2$.[29]

Particle images were obtained using a Zeiss EM 10 transmission electron microscope (TEM). The particles were collected by placing a droplet of the solution on a nickel TEM grid.

Results and Discussion

The formation of copper nanoparticles via reduction of $CuAOT_2$ within AOT reverse micelle systems was monitored in-situ using time-resolved UV−Vis absorption measurements.

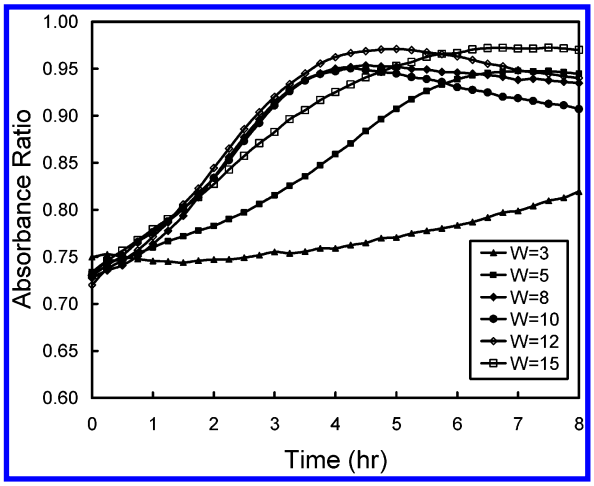

Figure 4. Cu nanoparticle growth curves measured in-situ by (Abs_{500}/Abs_{566}) as a function of time using an isooctane bulk solvent and adjusting the W value with [AOT] = 0.1106 M, [$CuAOT_2$] = 0.01106 M, N_2H_4 = 3X [Cu].

TABLE 1: Experimental Results of the Relative Particle Growth Rates and Maximum Particle Sizes Obtained for Copper Nanoparticles Synthesized in Various Alkane Bulk Solvents with [$CuAOT_2$] = 0.01106 M, [AOT] = 0.1106 M, and $W = 5$ and 10[a]

	$W = 5$			$W = 10$			calculations
solvent	size (nm)	slope ± 95%	R^2 (%)	size (nm)	slope ± 95%	R^2 (%)	size (nm)
pentane	8.3	1.74 ± 0.14	93.4	8.6	1.16 ± 0.08	90.5	10.6
hexane	8.6	1.62 ± 0.17	81.4	8.9	1.87 ± 0.20	91.4	11.1
heptane	8.6	1.36 ± 0.13	72.4	8.6	1.44 ± 0.08	96.7	11.5
octane	8.5	1.96 ± 0.15	92.0	8.4	1.39 ± 0.10	93.3	11.8
decane	9.1	1.77 ± 0.17	84.5	8.9	1.85 ± 0.12	94.0	12.2
dodecane	9.0	2.00 ± 0.19	87.6	9.7	2.31 ± 0.49	36.4	12.6
isooctane	9.4	1.25 ± 0.10	86.5	9.6	2.11 ± 0.18	97.8	11.3
cyclo-hexane	12.6	1.09 ± 0.27	59.6	12.6	1.55 ± 0.38	76.1	12.8

[a] The calculation results obtained from the total interaction energy model show excellent agreement with the maximum particle sizes obtained experimentally.

The relative growth rates and maximum particle sizes are obtained from these absorbance measurements using the relationship established for the absorbance ratio (Abs_{566}/Abs_{500}) versus particle size developed by Lisiecki and Pileni.[12] This study presents an investigation of the effects of bulk solvent type and water content, W, on the particle growth rate and maximum particle size in conventional liquids.

The relative growth rate is determined from the initial 3 to 4 hours of particle growth obtained from a plot of Abs_{566}/Abs_{500} as a function of time, shown in Figures 2−4. Quantitative representation of the relative particle growth rates based on the absorption measurements are listed in Tables 1 and 2 as the slope of the particle size vs time plots, where the particle sizes are obtained from the Abs_{566}/Abs_{500} by the relationship mentioned previously.[18] The slope was determined by a linear regression analysis of multiple experimental growth curves for each of the bulk solvents and W values. How well the regression analysis fits the particle growth curves is represented by an R^2 value. The error in the particle growth rate represented by the slope is determined from a 95% confidence interval calculated by twice the standard error obtained from the regression analysis. The maximum particle size is obtained from the maximum absorbance ratio (Abs_{566}/Abs_{500}) observed throughout each experiment.

TABLE 2: Experimental Results of the Relative Particle Growth Rates and Ultimate Particle Sizes Obtained for Copper Nanoparticles Synthesized in an Isooctane Reverse Micelle System with [$CuAOT_2$] = 0.01106 M and [AOT] = 0.1106 M for *W* Values Ranging from 3 to 15

isooctane	diameter (nm)	slope ± 95%	R^2 (%)
$W = 3$	10.5	0.14 ± 0.03	79.9
$W = 5$	9.4	1.25 ± 0.10	86.4
$W = 6.5$	9.1	1.91 ± 0.24	88.8
$W = 8$	9.7	2.23 ± 0.18	93.5
$W = 10$	9.6	2.11 ± 0.18	94.9
$W = 12$	10.7	2.35 ± 0.18	96.0
$W = 15$	10.8	1.64 ± 0.17	92.7

Figure 2 is a plot of the absorbance ratio (Abs_{566}/Abs_{500}) measured as a function of time where each curve represents an average of between 2 and 10 particle growth measurements in each solvent with $W = 5$ (only the results from the even-carbon-number solvents are shown for clarity). In analyzing the particle growth curves in each liquid solvent, the particle growth in isooctane and cyclohexane is slower than all of the straight chain hydrocarbons at a water content of 5. Figure 2 illustrates that for the *n*-alkane solvents there is only a very slight increasing trend in the growth rate with an increase in carbon number. Similar results are observed for the maximum particle sizes obtained in each solvent as shown in Table 1. The maximum particle size shows a general increase in particle size as the carbon chain increases in length with a maximum size of 8.3 nm in pentane and a maximum size of 9.0 nm in dodecane. Larger particle sizes were obtained in both isooctane (9.4 nm) and cyclohexane (12.6 nm) solvents compared to all of the *n*-alkane solvents. This suggests that growth rate and particle size are inversely related where a decrease in growth rate corresponds to a larger maximum particle size at a specific *W* value. Increased interaction between the solvent and the surfactant tails results in a more stable micelle system and an enhanced ability to stabilize larger particles while reducing the intermicellar exchange.

Previous investigations by other researchers on the effects of the bulk alkane solvent on the AOT reverse micelle system have produced results that support these findings.[2,4,9,16] Considerable work has been done to gain a better understanding of CdS nanocrystal growth where Towey states that particle formation is controlled to an extent by the nature of the continuous phase, where the growth rate increases from cyclohexane to *n*-heptane to *n*-decane.[7] Bagwe demonstrated with the production of silver and silver chloride particles that an increased intermicellar exchange rate has the effect to increase the growth rate and more importantly decrease the final particle size.[16,17] These results are explained by the solvent−tail interactions or more generally, a decrease in the rigidity of the micelle.

Also of interest is the influence of *W* on the particle growth rate and maximum particle size. Figure 3 represents the particle growth curves for the same alkane solvents as in Figure 2 with an increased $W = 10$. An interesting observation from this figure is that there is essentially no influence of the solvent on the particle growth rate within the experimental error at the increased water content value of 10. Previous studies[18] of copper particle growth as a function of bulk solvent type have demonstrated that the particle growth rate increases with increasing *W* from 5 to 10 in both isooctane and cyclohexane solvents. Additionally, Figure 3 and Table 1 show that the influence of *W* on the final particle size obtained is negligible. This shows that even though *W* may have some influence on the intermicellar exchange it is not the controlling factor for the maximum particle size obtained given sufficient reaction time. The solvent and its interaction with the surfactant tails, however, is a contributing factor for the stabilization of particles in solution and the maximum particle size obtainable. This study suggests a lesser effect of solvent chain length on the growth rate and the ultimate particle size for *n*-alkane solvents when compared to isooctane or cyclohexane. This observation is of particular interest and may be the subject of future experimentation. For the cyclohexane and isooctane solvents, it has been suggested that the solvent molecules will pack within the surfactant tails, creating a more rigid micelle and thus retarding the intermicellar exchange.[17]

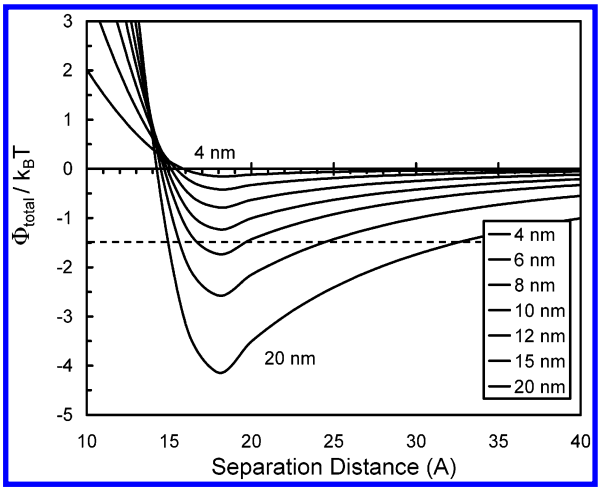

Figure 5. Plot of the Total Interaction Energy, Φ_{total}/k_BT, curves calculated for 4 nm to 20 nm diameter Cu nanoparticles coated with AOT and dispersed in hexane at 20 °C and 1 bar. The model predicts an ultimate particle size of ~9 nm in diameter for hexane.

Further investigation of the *W* effect on copper nanoparticle synthesis is shown in Figure 4 in the range of $W = 3$ to 15 for the isooctane/water/AOT system. Table 2 demonstrates that the particle growth rate goes through a maximum at approximately $W = 12$. The role of the water content in particle growth is of particular interest in the intermicellar exchange process and has been studied in several systems.[6,7,10,15,17,18] A similar maximum was presented by Atik and Thomas[2] where for low *W* values (for $W = 5.5$ to 11), an increase in water content leads to a decrease in the rigidity of the water region which in turn leads to a more rapid reaction rate. Continued increase of the water content, above $W = 11$, leads to a decrease in the reaction rate which was explained by Atik and Thomas through a decrease in local concentration of the reactants in the larger water cores. These trends observed for the reaction rate lead to a maximum in the intermicellar exchange rate as a function of the *W* value which corresponds to the particle growth rates observed in this study, a maximum at $W = 12$.

At low *W* values the water has been shown to hydrate the polar headgroup of the surfactants and is considered bound water. This provides a rigid water environment,[2] and differs significantly from a bulk water environment. Experimental instances where an increase in particle growth rate with increasing water content at low *W* values has been presented for AgCl,[17] CdS, and ZnS[15] nanoparticle formation which is attributed to the dynamics of the water environment and the intermicellar exchange rate of the reverse micelles. With an increase in *W*, ~ 10, the water core becomes free from the binding headgroups but still differs from bulk water and is considered to be intermediate water. As a result, the rigidity of the water decreases and an increase in reaction rate is observed. For larger *W*, ~ 20, a bulk water environment appears and a

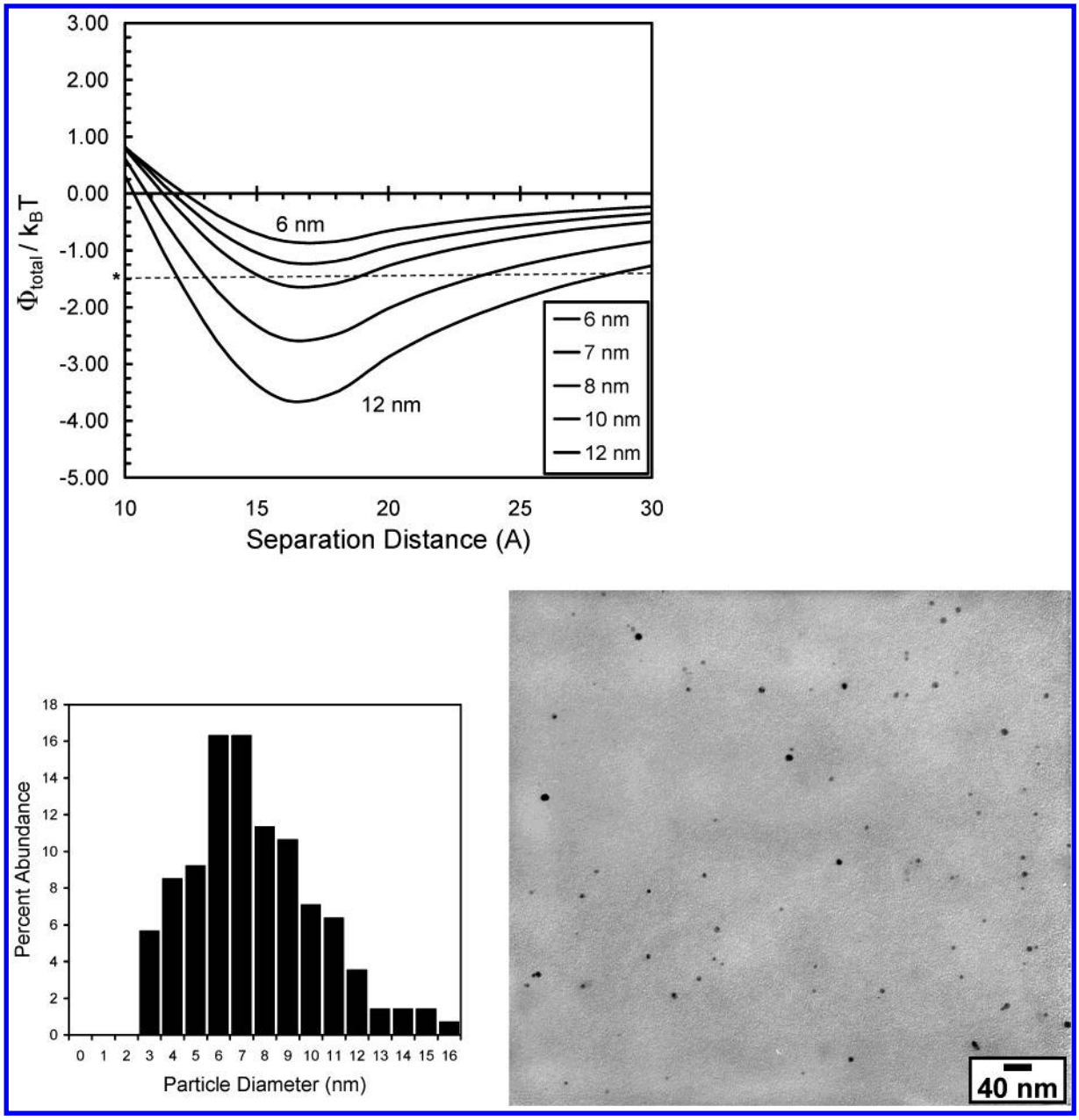

Figure 6. (a) Plot of the Φ_{total}/k_BT curves calculated for 6 nm to 12 nm diameter Ag nanoparticles coated with AOT and dispersed in hexane at 25 °C and 1 bar. (b,c) TEM image and size distribution for Ag particles synthesized in liquid hexane−AOT−water reverse micelle system with 1.0×10^{-3} M AgAOT, 9.9×10^{-2} M AOT, and $W = 10$.

decrease in intermicellar exchange is observed with increasing water content although, not as dramatic an effect as for lower W values. The decrease in intermicellar exchange rate at larger W values has been observed in a variety of systems[2,4,5] including the work previously mentioned by Atik and Thomas[2]. Several explanations for decrease in intermicellar exchange at larger W values have been presented. In particular, Fletcher et al.[4] explained the decreasing exchange rate for W values greater than 10 by an increase in the apparent activation energies for micelle exchange. This is associated with instances of structural states with interfacial regions of unfavorable surfactant film curvature in the range of W from 10 to 30. More recently, investigations by Goto and co-workers have examined the isooctane/water/AOT reverse micellar system and have found that at low W (∼2), the mobility of the water is significantly suppressed. It was also observed that at $W > 10$ there is an onset of the formation of loose aggregates of reverse micelles which is termed flocculation. The flocculation was shown to precede the onset of percolation which has been observed at higher AOT and water concentrations having the effect of forming more rigid and larger network structure of reverse micellar solutions.

While the growth rate of copper nanoparticles is influenced by the water content, there is no noticeable effect of W on the ultimate particle size obtained in a given solvent. In fact, 10 nm diameter particles are obtained from 3 nm diameter reverse micelles for a $W = 10$ (reverse micelle radius r(Å) = 1.5 W) suggesting that the ultimate particle size is not controlled simply by a micelle core templating effect. This supports a theory that the surfactant has multiple functionality in the particle growth and stabilization process. Initially the surfactant provides an initiation site, the micelle core, for the reduction of the metal followed by particle growth through intermicellar exchange, and at the latter end of the particle growth the surfactant acts as a stabilizing ligand with a weak interaction energy between the metal particle and the surfactant headgroup. The results from

the isooctane system, shown in Table 2 and Figure 4, show that given enough reaction time, *W* has negligible effect on the maximum particle size. This suggests that the surfactant and bulk solvent, rather than *W*, more strongly influence the ultimate copper nanoparticle size obtained. These results will be explained below in terms of steric stabilization of the particles in a given solvent/surfactant system. This approach may provide insight as to whether the micelle core truly provides a template for particle growth or if steric stabilization controls the maximum particle size.

Various spectroscopy and imaging techniques have been utilized to determine the geometry and structure of the micelles with a variety of surfactant systems. The surfactants act to stabilize the water core, creating a minimum energy environment forming a most desirable geometry. In the same respect, particles formed in these systems are built from smaller particles down to the atomic level and the surfactants act to sterically stabilize the growing particle, conforming to a similar geometry. Depending on the strength of the solvent−tail interactions, the particles will continue to grow until they are no longer sterically stabilized, thus allowing for particle sizes to exceed the size of the original micelle.

In some specific cases, researchers have found the sizes of particles synthesized in AOT reverse micelles can in fact correlate with the size of the reverse micelle core (core size is proportional to *W*). Examples include CdS, ZnS, AgCl, and CdTe.[10,13,15,17,30,31] However, in each of these cases, the particle sizes obtained rarely exceeded the size of the micelle core. The particles examined in these cases are not pure metals, and it is possible that a weaker interaction between the particle surface and the ionic headgroup of the surfactant exists, thus inhibiting the steric stabilization of particles larger than the micelle core. Sato et al.[30] demonstrated that the deposition of a Cd layer on the surfaces of CdS particles synthesized within AOT reverse micelles was required in order to attach a thiol ligand for particle separation and imaging. Additional work is required to provide further evidence of interactions between the metallic nanoparticles and the ionic surfactant headgroups.

Modeling Results

The previous discussion reveals that the bulk solvent type has an effect on the stabilization of various particle sizes which can be described by the solvent−surfactant tail interactions. The proposed interaction energy model provides a quantitative explanation for the maximum particle sizes obtained in various solvents by balancing the attraction and repulsion forces between AOT-covered particles interacting in a bulk solvent. Figure 5 exhibits the results of the total interaction energy calculations for copper nanoparticles coated with AOT surfactant as a function of the separation distance and particle size at 20 °C and 1 bar in hexane. From Table 1, the model predicts maximum particle diameters in a range of solvents including a diameter of 10.6 nm in pentane through a diameter of 12.8 nm in cyclohexane. The calculated maximum particle diameters correspond well with the experimental results at *W* values of 5 and 10 in Table 1. Comparison of the experimental particle sizes and the model predictions shows good agreement for the solvent cyclohexane with a maximum particle size of 12.6 nm. The model predicts smaller maximum particles sizes in all of the *n*-alkane solvents studied compared to the cylcohexane predictions with increasing particle size from 9.8 to 12.1 nm with increasing carbon number. The model predicts slightly larger particles in each of the alkane solvents compared to the experimental results obtained from the UV−Vis measurements.

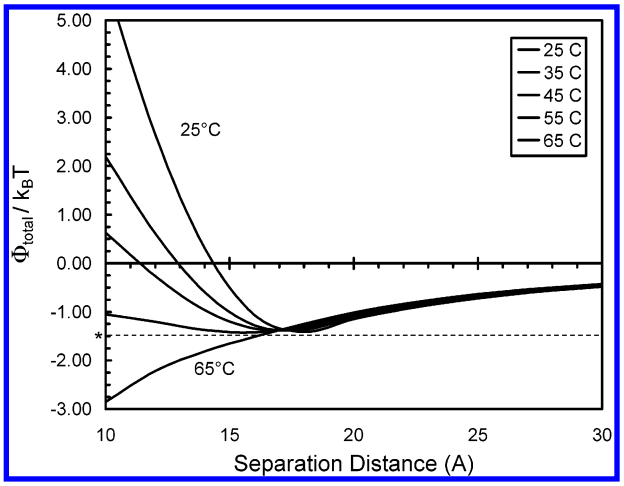

Figure 7. Plot of the Φ_{total}/k_BT curves calculated for 10 nm diameter Cu nanoparticles coated with AOT and dispersed in hexane at 1 bar and temperatures ranging from 25 °C to 65 °C. The model predicts that 10 nm diameter Cu particles would be sterically stabilized in hexane at 25 °C; however, as the temperature is increased to 65 °C the particles would agglomerate and precipitate out of solution.

The experimental results show particle sizes ranging from 8.3 to 9.7 nm from pentane to dodecane; however, the maximum particle size trend predicted by the model is more significant. From the calculations it would be expected that larger particles would be obtained for the larger alkanes although additional properties not accounted for by the model may contribute to instability in the micellar system resulting in the smaller sizes observed in the experimental results. Fletcher et al.[4] discuss that for the decane and dodecane systems, the experimental conditions explored in this study approach an upper phase transition where it has been shown that clustering of AOT-stabilized droplets in dodecane occurs around 25 °C and above. A SANS structure-factor analysis in the vicinity of this region reveals a sharp increase in additional short-range attractive interactions. If this attractive interaction were accounted for by the model, then it would have the effect of lowering the total interaction energy curve in the region $h < 2l$; this would result in a particle size smaller than what is predicted by the model, thereby more closely relating to the experimental data.

Figure 6a demonstrates that this model is also applicable to the synthesis of silver particles in hexane/AOT reverse micelle systems, which predicts a maximum particle size of ∼7.5 would be synthesized. Figure 6b,c is a TEM image and particle size distribution of silver nanoparticles synthesized in a hexane solution with [AgAOT] = 0.001M, [AOT] = 0.099M, and $W = 10$, where the majority of the silver nanoparticles are 6 to 7 nm in diameter, corresponding directly to the predictions of the model.

Other properties of the system that the model takes into account which affect the predicted ultimate particle size include temperature and percentage of particle surface coverage by the surfactant. Figure 7 shows the effect of temperature on 10 nm copper particles in hexane where the ability to sterically stabilize the particles becomes increasingly difficult as the temperature increases to 65 °C where the particles would no longer be supported. The same effect of temperature was observed by Shah et al.[21] where an increase in temperature requires an increase in pressure of the SCF ethane to obtain an adequate solvent interaction parameter in order to selectively separate silver nanoparticles. Figure 8 shows the effect of decreasing particle surface coverage from 90% to 30% which largely influences the surfactant volume fraction calculated in eq 9. As the

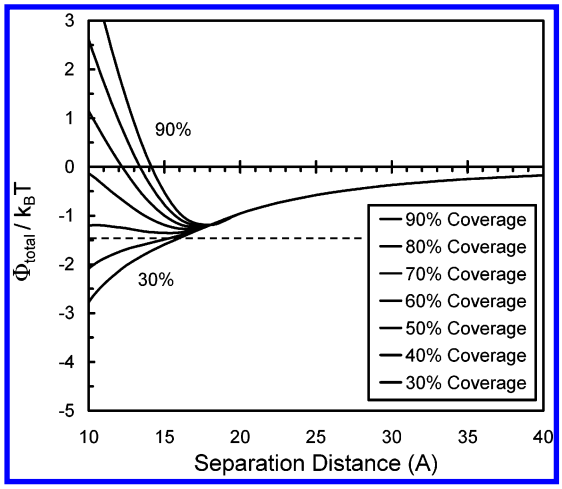

Figure 8. Plot of the Φ_{total}/k_BT curves calculated for 8 nm diameter Ag nanoparticles coated with AOT and dispersed in hexane at 20 °C and 1 bar with decreasing surface coverage of AOT on the Ag particles. The model predicts that as the percent surface coverage decreases, the ability to stabilize particles in solution also decreases.

surfactant surface coverage decreases below 50% for silver particles in hexane, the particles would no longer be sterically stabilized by the surfactant. The effect of surface coverage has bearing on the previously mentioned case for particles consisting of multiple atomic species.[7,13−15,17,30,31] The inability of the ionic headgroup to interact with the particle surface directly would effectively lower the particle surface coverage and thus restrict particle growth beyond the size of the micelle. This may explain the occurrence of purely metallic particles exceeding the size of the original micelle where the AOT surfactant acts to sterically stabilize the particles in solution, allowing for growth beyond the size of the water core. Further work will investigate the interaction forces between the particle surface and the ionic surfactant headgroup to better understand the mechanism of steric stabilization of metallic nanoparticles in the AOT reverse micelle system.

Conclusions

This study demonstrates that, for the synthesis of copper nanoparticles within the AOT reverse micelle system, the bulk organic phase influences both the particle growth rate and ultimate particle size obtained. The size of the micelle, determined by *W*, significantly affects the particle growth rate, which goes through a maximum at $W = 12$, but given adequate reaction time, *W* does not have an effect on the ultimate particle size obtained. This leads to the conclusion that surfactant templating is not the particle size determining factor, but rather steric stabilization of the particles by the AOT surfactant is responsible for the particle size and geometry synthesized. The total interaction energy model takes a simplistic approach modeling the metallic particles coated with AOT surfactant as soft spheres, calculating the attractive van der Waals forces acting between the metallic particles and the repulsive osmotic and elastic forces which result from the tail−tail and solvent−tail interactions responsible for the steric stabilization of the metallic particles. Results from the model accurately predict the ultimate copper and silver particle sizes obtained experimentally in the various alkane solvents.

Acknowledgment. We thank Dr. Micheal Miller of the Auburn University Research and Instrumentation Facility for his assistance with TEM analysis. The authors would also like to thankfully acknowledge financial support from the Department of Energy—Basic Energy Sciences (DE-FG02-01ER15255).

References and Notes

(1) Nave, S.; Eastoe, J.; Heenan, R. K.; Steytler, D.; Grillo, I. *Langmuir* **2000**, *16*, 8741.
(2) Atik, S. S.; Thomas, J. K. *J. Am. Chem. Soc.* **1981**, *103*, 3543.
(3) Eicke, H. F.; Shepherd, J. C. W.; Steinemann, A. *J. Colloid Interface Sci.* **1976**, *56*, 168.
(4) Fletcher, P. D. I.; Howe, A. M.; Robinson, B. H. *J. Chem. Soc., Faraday Trans. I* **1987**, *83*, 985.
(5) Howe, A. M.; McDonald, J. A.; Robinson, B. H. *J. Chem. Soc., Faraday Trans. I* **1987**, *83*, 1007.
(6) Natarajan, U.; Handique, K.; Mehra, A.; Bellare, J. R.; Khilar, K. C. *Langmuir* **1996**, *12*, 2670.
(7) Towey, T. F.; Khanlodhi, A.; Robinson, B. H. *J. Chem. Soc., Faraday Trans.* **1990**, *86*, 3757.
(8) Tojo, C.; Blanco, M. C.; Rivadulla, F.; Lopez-Quintela, M. A. *Langmuir* **1997**, *13*, 1970.
(9) Binks, B. P.; Kellay, H.; Meunier, J. *Europhys. Lett.* **1991**, *16*, 53.
(10) Sato, H.; Hirai, T.; Komasawa, I. *Ind. Eng. Chem. Res.* **1995**, *34*, 2493.
(11) Pileni, M. P. *Langmuir* **1997**, *13*, 3266.
(12) Lisiecki, I.; Pileni, M. P. *J. Phys. Chem.* **1995**, *99*, 5077.
(13) Petit, C.; Lixon, P.; Pileni, M. P. *J. Phys. Chem.* **1990**, *94*, 1598.
(14) Hirai, T.; Tsubaki, Y.; Sato, H.; Komasawa, I. *J. Chem. Eng. Jpn.* **1995**, *28*, 468.
(15) Hirai, T.; Sato, H.; Komasawa, I. *Ind. Eng. Chem. Res.* **1994**, *33*, 3262.
(16) Bagwe, R. P.; Khilar, K. C. *Langmuir* **2000**, *16*, 905.
(17) Bagwe, R. P.; Khilar, K. C. *Langmuir* **1997**, *13*, 6432.
(18) Cason, J. P.; Miller, M. E.; Thompson, J. B.; Roberts, C. B. *J. Phys.Chem. B* **2001**, *105*, 2297.
(19) Cason, J. P.; Khambaswadkar, K.; Roberts, C. B. *Ind. Eng. Chem. Res.* **2000**, *39*, 4749.
(20) Eastoe, J.; Warne, B. *Curr. Opin. Colloid Interface Sci.* **1996**, *1*, 800.
(21) Shah, P. S.; Holmes, J. D.; Johnston, K. P.; Korgel, B. A. *J. Phys. Chem. B* **2002**, *106*, 2545.
(22) Eichenlaub, S.; Chan, C.; Beaudoin, S. P. *J. Colloid Interface Sci.* **2002**, *248*, 389.
(23) Israelachvili, J. N. *Intermolecular and surface forces: with applications to colloidal and biological systems*; Academic Press: London, Orlando [FL], 1985.
(24) Lide, D. R. *Handbook of Organic Solvents*; CRC: Boca Raton, FL, 1995.
(25) Vincent, B.; Edwards, J.; Emmett, S.; Jones, A. *Colloids Surf.* **1986**, *18*, 261.
(26) Fried, J. R. *Polymer Science and Technology*; Prentice Hall: Englewood Cliff, NJ, 1995.
(27) Smith, J. M.; Van Ness, H. C.; Abbott, M. M. *Introduction to chemical engineering thermodynamics*, 5th ed.; McGraw-Hill: New York, 1996.
(28) Eastoe, J.; Fragneto, G.; Robinson, B. H.; Towey, T. F.; Heenan, R. K.; Leng, F. J. *J. Chem. Soc.,Faraday Trans.* **1992**, *88*, 461.
(29) Petit, C.; Lixon, P.; Pileni, M. P. *J. Phys. Chem.* **1993**, *97*, 12974.
(30) Sato, H.; Asaji, N.; Komasawa, I. *Ind. Eng. Chem. Res.* **2000**, *39*, 328.
(31) Feltin, N.; Levy, L.; Ingert, D.; Pileni, M. P. *J. Phys. Chem. B* **1999**, *103*, 4.